DOI: http://dx.doi.org/10.15407/tpwj2018.11–12.16

EFFECT OF MULTI-PASS FRICTION STIR PROCESSING ON THE MICROSTRUCTURE AND MECHANICAL PROPERTIES OF DUAL PHASE STEEL

T. KÜÇÜKÖMEROĞLU[1], **S.M. AKTARER**[2], **G. İPEKOĞLU**[3] and **G. ÇAM**[3]
[1]Department of Mechanical Engineering, Karadeniz Technical University, Trabzon, Turkey. E-mail: tkomer@ktu.edu.tr
[2]Department of Automotive Technology, Recep Tayyip Erdogan University,
Rize, Turkey. E-mail: semih.aktarer@erdogan.edu.tr
[3]Department of Mechanical Engineering, Iskenderun Technical University,
31200 İskenderun-Hatay, Turkey. E-mail: guven.ipekoglu@iste.edu.tr; gurel.cam@iste.edu.tr

Dual phase (DP) steels have been widely used in the automotive industry due to the excellent engineering properties such as high strength and good formability. However, attempts have recently been ongoing to improve their mechanical and formability properties in order to achieve further weight savings. Mechanical and microstructural properties of DP steel can be improved by severe plastic deformation (SPD) techniques without changing their chemical compositions. Among SPD methods, friction stir processing (FSP) is a new method used to enhance the properties of plate and/or sheet types of metals. Therefore, the effect of multi-pass FSP (M-FSP) on the microstructure and mechanical performance of a DP steel (i.e., DP600) was investigated in the current study. M-FSP was applied to dual phase steel at the 4mm steps. FSP resulted in a refined microstructure which brought about a considerable increase in both hardness and strength values. After FSP, islands of martensite as the secondary phase in the microstructure have been broken and disturbed by the rotational pin. The processed region consists of ferrite, bainite and martensite. The hardness value increased from 210 $HV_{0.2}$ to about 360 $HV_{0.2}$ after M-FSP. 36 Ref., 1 Table, 4 Figures.

Keywords: *friction stir processing, dual-phase steel, fine grained microstructure, mechanical properties*

Introduction. Dual Phase (DP) steels are widely used in the automotive industry due to their excellent mechanical properties such as high strength and good formability [1–3]. However, numerous studies have recently been conducted to improve the strength and ductility of these steels which in turn further reduce the weight and ensure safety [4–6]. The mechanical properties of DP steels can be improved by severe plastic deformation (SPD) techniques without changing their chemical compositions [7, 8]. Friction stir processing (FSP) is a novel SPD method which can be used for the improvement of properties. It can even be said that friction stir process is the most ideal method among the SPD methods when considering the processing of large scale plate or sheet type materials [9].

FSP is based on the basic principles of friction stir welding (FSW) [10], which is originally developed for joining difficult-to-weld Al-alloys [11–14]. FSP is a method of improvement of the properties of a material by way of severe, localized plastic deformation which is produced by immersing a non-consumable tool into the work piece, and rotating and traveling the tool in a stirring motion [15]. Many review papers on this process have been published until now, and thus detailed information on its principles can be obtained in Refs. [16–19]. As the FSP deforms a limited region, the multi-pass FSP, which is applied sequentially, leads to deformation of larger regions and allows material properties to be improved in large-scale dimensions. Up to now, multi-pass FSP has been applied to mostly aluminum alloys [20–25] and few magnesium alloys [26–28] and pure titanium [29]. Generally, it was reported that multi-pass FSP improves mechanical properties of cast Al alloys containing Si and achieves significant microstructural refinement [25, 30–32]. Aktarer et al. [33] reported that two-pass FSP of Al12Si alloy leads to fragmentation of needle-shaped silicon plates from 27±23 μm to about 2.6±2.4 μm, thus both strength and ductility are remarkably increased, i.e., about 1,3 and 7 times than that of base metal, respectively. Similarly, Lua et al. showed that multi-pass FSP significantly improved both strength and ductility of cast magnesium alloys such as AZ61 due to grain refinement and the elimination of cast defects [26]. Also, corrosion behavior of multi-pass friction stir processed (FSP) pure titanium was investigated by Fattah–Alhosseini et al. [29]. They found that grain refinement in the multi-pass FSPed sample led to a reduction in both corrosion and passive current densities.

Although there are many reports on multi-pass FSP (M-FSP) of non-ferrous alloys and single-pass FSP of steels [33, 34], only limited amount of studies have been undertaken systematically on the (M-FSP)

© T. KÜÇÜKÖMEROĞLU, S.M. AKTARER, G. İPEKOĞLU and G. ÇAM, 2018

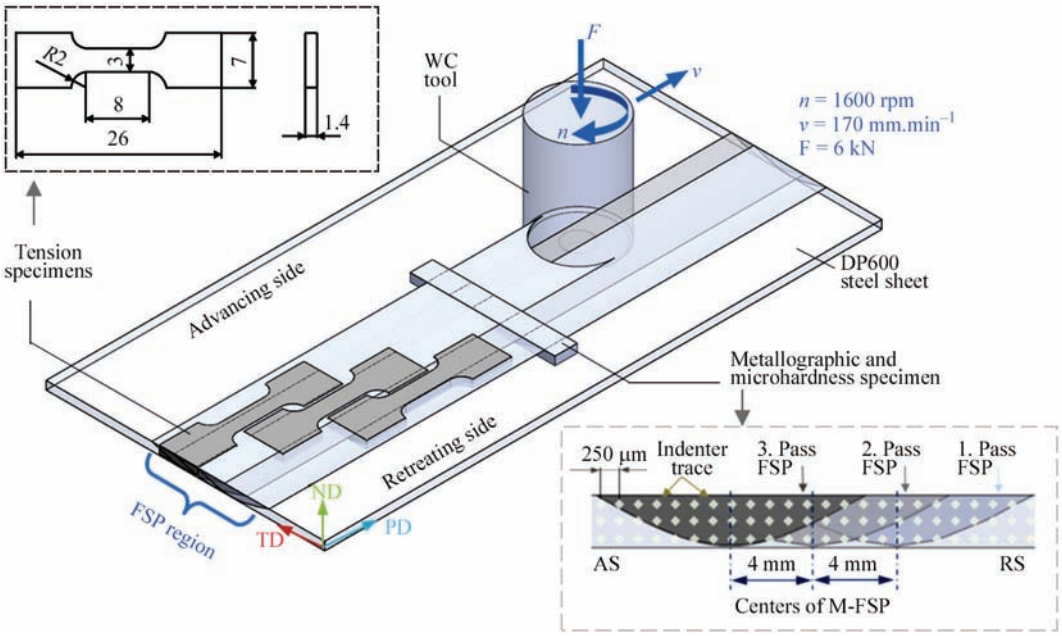

Figure 1. Schematic illustration of M-FSP technique which shows the specimens' geometries extracted from the FSPed sheet and the position from which they were extracted

of steels. Furthermore, more studies are needed for getting further improvement in mechanical properties of multi-pass friction stir process of dual phase steel. Therefore, the main purpose of this study is to determine the effect of multi-pass FSP on the microstructural evolution, microhardness and tensile properties of a dual phase steel (i.e., DP600).

Experimental procedure. Hot rolled DP600 steel with a chemical composition of 0.040 % C, 1.436% Mn, 0.239 % Si, 0.047 % Al, 0.035 % Cu, 0.690 % Cr, 0.039 % Ni, 0.011 % Mo and balance Fe was used in this study. Samples with the dimensions of 200×50 mm×1.5 mm were cut from the steel plate for multi-pass friction stir processing (M-FSP). M-FSP was performed with a processing tool having a flat shoulder with the diameter of 14 mm and a cylindrical pin with the diameter and length of 5 mm and 1.3 mm, respectively. In FSP trials, a tool rotational rate of 1600 rpm and a traverse speed of 170 mm/min were used. The shoulder tilt angle was set at 2°, and the tool downforce was kept constant at 6 kN during process. The subsequent M-FSP was shifted toward the advancing side with stepping of 4mm, thus a total of 3 overlapping passes were carried out on the DP600 steel sheet. Schematic illustration of M-FSP process is shown in Figure 1.

Optical microscopy (OM) and scanning electron microscopy (SEM) were used to observe the microstructure of the samples before and after M-FSP. The metallography specimens were extracted perpendicular to the processing direction (Figure 1), polished with standard techniques and then etched in % 2 Nital (3ml. HNO_3 + 97 ml. C_2H_6O) for 20 s. Mechanical properties of the base and M-FSPed samples were determined using tensile test and hardness measurements. Dog-bone shaped tensile test specimens with the gauge dimensions of 1.4×3×8 mm were extracted from the base material and M-FSPed plates by electro discharging machining (EDM) technique. These specimens were cut parallel to the process direction at three different positions inside the FSPed region as shown in Figure 1. The positions of the tensile test specimens are representative of the center of each pass FSP region shifted to 4 mm steps. The tests were performed using an electro-mechanical load frame with a video type extensometer at a strain rate of $5 \cdot 10^{-4}$ s^{-1}. Vickers micro-hardness tests were carried out using a load of 200 g and a dwell time of 10 s. Vickers microhardness measurements were conducted throughout the cross section of the processed specimen with an interval of 250 µm as illustrated in Figure 1.

Results and discussion. *Microstructure.* Optical micrographs showing the microstructures of DP600 steel base plates are given in Figure 2. The initial microstructure of DP600 steel sheet is consisted of elongated ferrite grains in rolling direction and dispersed martensite throughout ferrite grain boundaries. Average ferrite grain size was 6 µm and the volume fraction of martensite was determined to be approximately 24 %. Martensite islands appear dark in optical micrograph (Figure 2, *a*) and they seem bright in SEM image (Figure 2, *b*).

An optical macrograph of M-FSPed region is given Figure 3, *a*, and the traces of the side-by-side pass are clearly visible. Final pass processed microstructure is shown in Figure 3, *b*, which is almost entirely lath martensite. This zone is seen as a darker region in macrograph. The region exhibits a similar characteristic to single-pass FSP microstructures. Since the process does not continue then there is no heat or de-

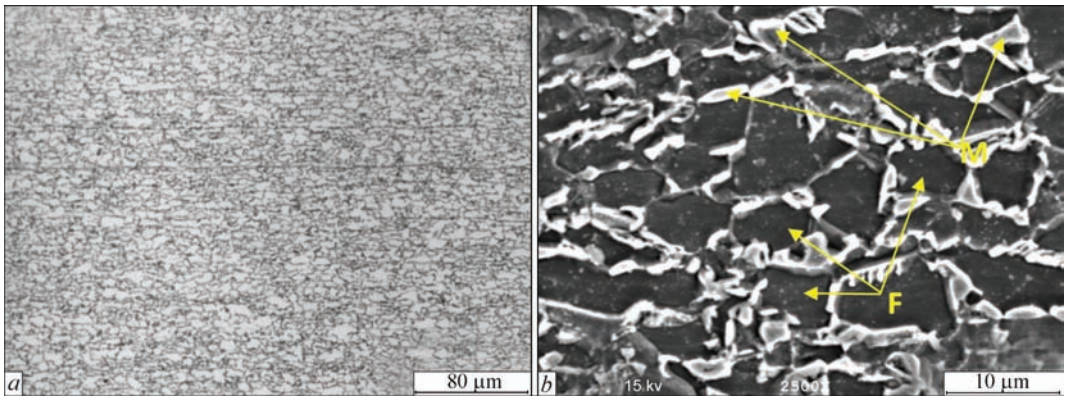

Figure 2. Micrographs showing the microstructure of DP600 steel base plate: *a* — optical micrograph; *b* — SEM image

formation to affect this region. However, it is a fact that the heat and deformation of the 2nd pass process affects the 3rd processed zone and it can be separated into single pass FSP. The lath martensite formed in the microstructure shows that this region is completely austenite during the process. Therefore, it can be said that the process temperature is above the A3 temperature line. Miles et al. [35] is reported that lath martensite is observed in SZ of friction stir welded DP590 steel. The microstructure in the SZ of the second pass process is shown Figure 3, *c*, which also corresponds to the heat affected zone of the third process. Therefore, while microstructure of this region is fully lath martensite after the 2nd pass process, it is transformed to acicular products by heat generated by the 3rd pass process. This microstructure consists of lath martensite and dispersed acicular and globular cementite through the ferrite matrix as seen Figure 3, *c*. The SZ of 1st pass process is actually the heat affected zone of 2nd pass process and its microstructure is given Figure 3, *d*. A predominantly bainitic structure is observed in this region, and the formation of various types of acicular products depends on the peak temperature, the cooling rate and the rate of deformation during the process. Kang et al. [36] reported that microstructures of bainite and martensite may form at different cooling rates in FSPed low-alloy high-strength steel. Their results clearly showed that the

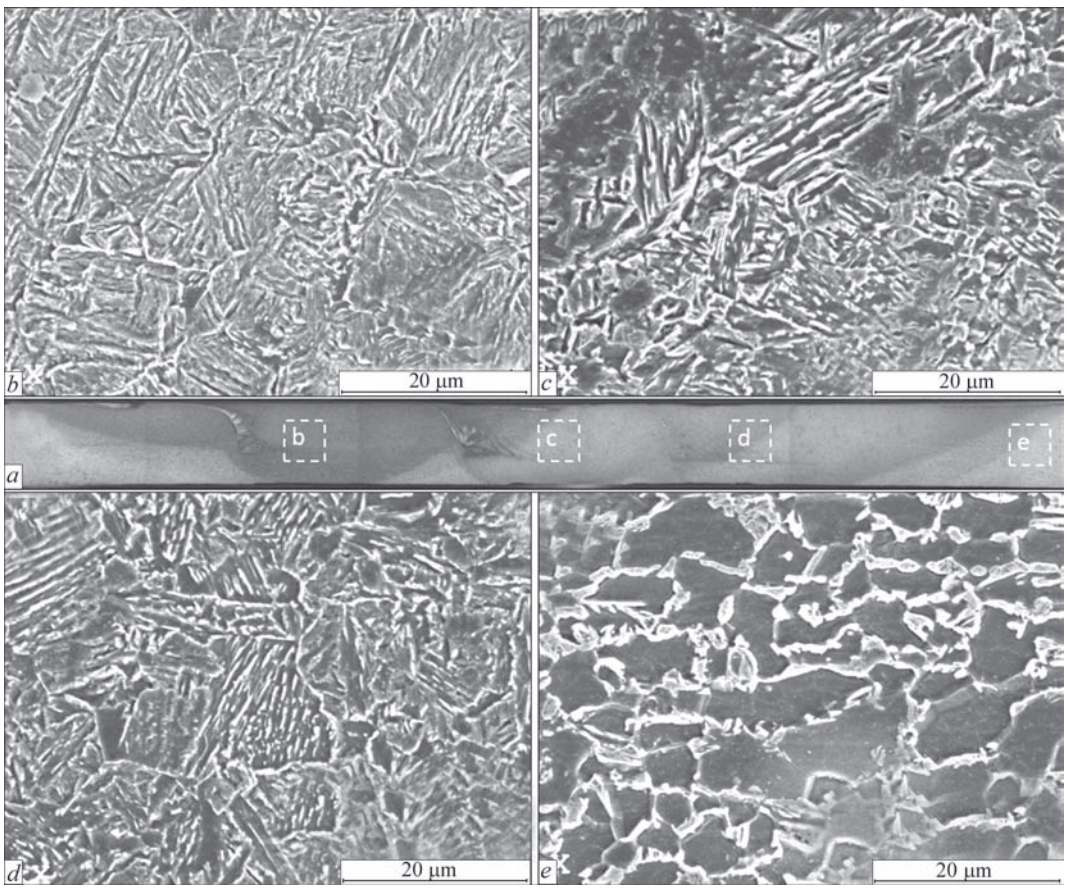

Figure 3. Optical macrograph of the cross-section of M-FSPed specimen (*a*), the SZ center of 3rd pass (*b*), the SZ center of 2nd pass (*c*), the SZ center of 1st pass (*d*), heat affected zone (HAZ) of 1st pass at the retracting side (*e*)

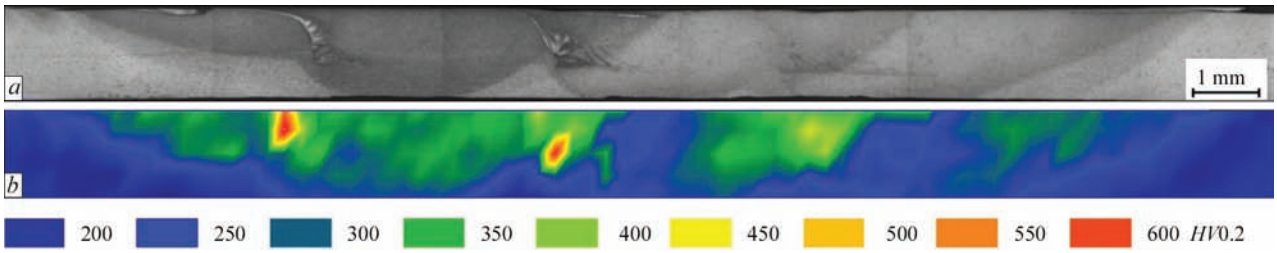

Figure 4. Optical microstructure of cross section of the M-FSPed sample extracted perpendicular to the process direction (*a*); a contour map showing the hardness distribution across the M-FSPed region (*b*)

microstructure comprises of completely bainite at a cooling rate of 30 °C/s and dominantly martensite at a cooling rate of 70 °C/s.

The microstructure of HAZ of 1st pass process at the retracting side is tempered martensite which consists of very small and uniformly dispersed cementite [37]. Figure 3(c) shows tempered martensite partially decomposing into cementite and ferrite from martensite islands in the HAZ.

Microhardness and tensile prosperities. The microhardness profile showing the hardness distribution across the M-FSPed region is given in Figure 4. The DP 600 steel base plate has a hardness of 210 *HV*. The highest hardness in the processed zone is approximately 550 *HV*, which is measured around the pin. The average hardness value of the stir zone corresponding to the rotating pin diameter is seen as the green region in the hardness map of 360 *HV*. This region corresponds to the volume of the rotating pin diameter and is also an important indication of material flow during FSP. This region has a lath martensitic microstructure with a homogeneous distribution. The stir zone of 1st pass process is affected by the heat generated by the next pass process, and the hardness drop in this zone is clearly observed with a light blue color. A similar characteristic feature is observed in the second pass process and each process is affected by the heat of the next pass process, and the hardness at the end decreases down to 250–300 *HV*. The microstructure of this transition region is a predominantly bainitic structure consisting of cementite and ferrite. The HAZ microstructure of retreating side is tempered martensite and this microstructure has 200 *HV* hardness in a very narrow region of about 250 μm. Since the hardness profile represents the dark blue 200–250 *HV* micro hardness range in the color mapping, the hardness decrease in the tempered martensite is not clearly visible.

The tensile test results of DP 600 steel before and after M-FSP are summarized in Table. DP 600 steel base plate sample displayed a high elongation with a large strain hardening region which is a typical characteristic of dual phase steels. The yield strength and ultimate tensile strength of base plate were 412 and 615 MPa, respectively. On the other hand, the SZs of 1st pass, 2nd pass and 3rd pass processed

Main strength and ductility values of each stir zone after M-FSP

Samples	Yield strength, MPa	Ultimate tensile ttrength, MPa	Elon-gation, %
DP 600	412	655	28
SZ of 1. Pass	321	560	30
SZ of 2. Pass	349	555	31
SZ of 3. Pass	657	830	25

samples exhibited yield strength values of 321, 349 and 657 MPa, respectively, and the ultimate tensile strength values of 560, 555 and 830 MPa, respectively. The low strength values exhibited by the SZs of 1st pass and 2nd pass FSPed samples compared to that of the base plate may be attributed to the fact that the microstructures of these samples transformed from initial martensite-ferrite structure to a predominantly bainitic structure. As seen from Table 1, no significant decrease in elongation was observed after M-FSP and all the specimens exhibited similar elongation values to that of the base plate.

Conclusions

Multi-pass friction stir process (M-FSP) technique was applied to DP 600 steel and their microstructural and mechanical properties of the M-FSPed plates have been investigated. The results of this study can be summarized as follows:

- the microstructure of the M-FSPed DP600 steel consists of lath martensite, bainite and recrystallized ferrite;
- it was observed that the next pass friction stir process affects the stir zone of the previous pass friction stir processed specimen. The heat generated by the next pass FSP leads to the transformation of lath martensite (formed after the previous pass FSP) to cementite and ferrite, thus results in a reduction in hardness;
- the hardness in the processed region increased to an average of 360 *HV* from 210 *HV* (hardness of base plate);
- the tensile strength values in the SZ of the first pass process and the second pass process were observed to be 560 and 555 MPa, respectively, both of which were lower than that of base plate (i.e., 655 MPa). This may be attributed to the tempering effect experienced in this regions. On the other hand, the tensile strength of the third process stir zone in-

creased to 830 MPa which is due to the existence of martensitic structure in this sample.

1. Rashid, M.S. (1981) Dual phase steels. *Ann. Rev. Mater. Sci*., **11**, 245–67.
2. Nıshımoto, A., Hosoya, Y., Nakaoka, K. (1981) A new type of dual-phase steel sheet for automobile outer body panels. *Transact. Iron Steel Inst. Japan*; **21**, 778–82.
3. Fonstein, N. (2017) *7 — Dual-phase steels*. Rana R, Singh SB, editors. Automot. Steels, Woodhead Publishing, 169–216.
4. Abid, N.H., Abu Al-Rub, R.K., Palazotto, A.N. (2017) Micromechanical finite element analysis of the effects of martensite morphology on the overall mechanical behavior of dual phase steel. *Int. J. Solids Struct*., **104–105**, 8–24.
5. Kundu, A., Field, D.P. (2016) Influence of plastic deformation heterogeneity on development of geometrically necessary dislocation density in dual phase steel. *Mater. Sci. Eng. A*, **667**, 435–43.
6. Ashrafi, H., Shamanian, M., Emadi, R., Saeidi, N. (2017) A novel and simple technique for development of dual phase steels with excellent ductility. *Ibid*., **680**, 197–202.
7. Son, Y Il, Lee, Y.K., Park, K.T. et al. (2005) Ultrafine grained ferrite-martensite dual phase steels fabricated via equal channel angular pressing: Microstructure and tensile properties. *Acta Mater*., **53**, 3125–34.
8. Park. K.-T., Lee, Y.K., Shin, D.H. (2005) Fabrication of ultrafine grained ferrite/martensite dual phase steel by severe plastic deformation. *ISIJ Int.*, **45**, 750–5.
9. Ma, Z.Y. (2008) Friction stir processing technology: A review. *Metall. Mater. Transact. A*, **39**, 642–58.
10. Mishra, R.S., Mahoney, M.W. (2007) Friction stir welding and processing. *ASM Int*., **368**.
11. Çam, G., İpekoğlu, G., Küçükömeroğlu, T., Aktarer, S.M. (2017) Applicability of friction stir welding to steels. *Journal of Achievements in Materials and Manufacturing Engineering*, 80(**2**), 65–85.
12. Çam, G., İpekoğlu, G. (2017) Recent developments in joining of aluminium alloys. *Int. J. Adv. Manuf. Technol*., 91(**5–8**), 1851–66.
13. Çam, G., Mıstıkoğlu, S. (2014) Recent developments in friction stir welding of Al-alloys. *Journal of Materials Engineering and Performance*, 23(**6**), 1936–53.
14. Çam, G. (2011) Friction stir welded structural materials: Beyond Al-alloys'. *Int. Mater. Rev*., 56(**1**), 1–48.
15. Mishra, R.S., Ma, Z.Y. (2005) Friction stir welding and processing. *Mater. Sci. Eng. R Reports*, **50**, 1–78.
16. Padhy, G.K., Wu, C.S., Gao, S. (2018) Friction stir based welding and processing technologies — processes, parameters, microstructures and applications: A review. *J. Mater. Sci. Technol*., **34**, 1–38.
17. Węglowski, M.S. (2018) Friction stir processing — state of the art. *Arch. Civ. Mech. Eng*., **18**, 114–29.
18. Chaudhary, A., Dev, A.K., Goel, A. et al. (2018) The mechanical properties of different alloys in friction stir processing: A review. *Mater. Today Proc*., **5**, 5553–62.
19. Sudhakar, M., Rao, C.H.S., Saheb, K.M. (2018) Production of surface composites by friction stir processing: A review. *Ibid*., 929–35.
20. Moustafa, E. (2017) Effect of multi-pass friction stir processing on mechanical properties for AA2024/Al_2O_3 nanocomposites. *Materials (Basel)*, **10**.
21. Chen, Y., Ding, H., Malopheyev, S. et al. (2017) Influence of multi-pass friction stir processing on microstructure and mechanical properties of 7B04-O Al alloy. *Transact. Nonferrous Met. Soc. China,* **27**, 789–96.
22. El-Rayes, M.M., El-Danaf, E.A. (2012) The influence of multi-pass friction stir processing on the microstructural and mechanical properties of aluminum Alloy 6082. *J. Mater. Proc. Technol*., **212**, 1157–68.
23. Nakata, K., Kim, Y.G., Fujii, H. et al. (2006) Improvement of mechanical properties of aluminum die casting alloy by multi-pass friction stir processing. *Mater. Sci. Eng. A*, **437**, 274–80.
24. Ramesh, K.N., Pradeep, S., Pancholi, V. (2012) Multipass friction-stir processing and its effect on mechanical properties of aluminum alloy 5086. *Metall. Mater. Transact. A Phys. Metall. Mater. Sci*., **43**, 4311–9.
25. Singh, S.K., Immanuel, R.J., Babu, S. et al. (2016) Influence of multi-pass friction stir processing on wear behaviour and machinability of an Al–Si hypoeutectic A356 alloy. *J. Mater. Proc. Technol*., **236**, 252–62.
26. Luo, X.C., Zhang, D.T., Zhang, W.W. et al. (2018) Tensile properties of AZ61 magnesium alloy produced by multi-pass friction stir processing: Effect of sample orientation. *Mater. Sci. Eng. A*, **725**, 398–405.
27. Xu, N., Bao, Y. (2016) Enhanced mechanical properties of tungsten inert gas welded AZ31 magnesium alloy joint using two-pass friction stir processing with rapid cooling. *Ibid*., **655**, 292–9.
28. Alavi Nia, A., Omidvar, H., Nourbakhsh, S.H. (2014) Effects of an overlapping multi-pass friction stir process and rapid cooling on the mechanical properties and microstructure of AZ31 magnesium alloy. *Mater Des*., **58**, 298–304.
29. Fattah-Alhosseini, A., Attarzadeh, F.R., Vakili-Azghandi, M. (2017) Effect of multi-pass friction stir processing on the electrochemical and corrosion behavior of pure titanium in strongly acidic solutions. *Metall. Mater. Transact. A Phys. Metall. Mater. Sci*., **48**, 403–11.
30. John Baruch, L., Raju, R., Balasubramanian, V. et al. (2016) Influence of multi-pass friction stir processing on microstructure and mechanical properties of die cast Al–7Si–3Cu aluminum alloy. *Acta Metall. Sin*., **29**, 431–40. Doi:10.1007/s40195-016-0405-2.
31. Meenia, S., Khan, M.D.F., Babu, S. et al. (2016) Particle refinement and fine-grain formation leading to enhanced mechanical behaviour in a hypo-eutectic Al–Si alloy subjected to multi-pass friction stir processing. *Mater. Charact*., **113**, 134–43.
32. Esmaily, M., Mortazavi, N., Osikowicz, W. et al. (2016) Influence of multi-pass friction stir processing on the corrosion behavior of an Al–Mg–Si alloy. *J. Electrochem. Soc*., **163**, C124–30.
33. Padhy, G.K., Wu, C.S., Gao, S. (2018) Friction stir based welding and processing technologies — processes, parameters, microstructures and applications: A review. *J. Mater. Sci. Technol*., **34**, 1–38.
34. Liu, F.C., Hovanski, Y., Miles, M.P. et al. (2018) A review of friction stir welding of steels: Tool, material flow, microstructure, and properties. *J. Mater. Sci. Technol*., **34**, 39–57.
35. Miles, M.P., Pew, J., Nelson, T.W., Li, M. (2006) Comparison of formability of friction stir welded and laser welded dual phase 590 steel sheets. *Sci. Technol. Weld. Join*., **11**, 384–8.
36. Kang, H.C., Park, B.J., Jang, J.H. et al. (2016) Determination of the continuous cooling transformation diagram of a high strength low alloyed steel. *Met. Mater. Int*., **22**, 949–55.

Received 16.07.2018